



CyTOF<sup>®</sup> XT. The neXT  
evolution in cytometry.

See what's neXT >



## Absence of Platelet Endothelial Cell Adhesion Molecule-1 (CD31) Leads to Increased Severity of Local and Systemic IgE-Mediated Anaphylaxis and Modulation of Mast Cell Activation

This information is current as of September 26, 2021.

Mae-Xhum Wong, Donna Roberts, Paul A. Bartley and Denise E. Jackson

*J Immunol* 2002; 168:6455-6462; ;  
doi: 10.4049/jimmunol.168.12.6455  
<http://www.jimmunol.org/content/168/12/6455>

**References** This article **cites 40 articles**, 24 of which you can access for free at:  
<http://www.jimmunol.org/content/168/12/6455.full#ref-list-1>

**Why *The JI*? Submit online.**

- **Rapid Reviews! 30 days\*** from submission to initial decision
- **No Triage!** Every submission reviewed by practicing scientists
- **Fast Publication!** 4 weeks from acceptance to publication

*\*average*

**Subscription** Information about subscribing to *The Journal of Immunology* is online at:  
<http://jimmunol.org/subscription>

**Permissions** Submit copyright permission requests at:  
<http://www.aai.org/About/Publications/JI/copyright.html>

**Email Alerts** Receive free email-alerts when new articles cite this article. Sign up at:  
<http://jimmunol.org/alerts>



# Absence of Platelet Endothelial Cell Adhesion Molecule-1 (CD31) Leads to Increased Severity of Local and Systemic IgE-Mediated Anaphylaxis and Modulation of Mast Cell Activation<sup>1</sup>

Mae-Xhum Wong, Donna Roberts, Paul A. Bartley, and Denise E. Jackson<sup>2</sup>

Platelet endothelial cell adhesion molecule-1 (PECAM-1) is a newly assigned member of the Ig-immunoreceptor tyrosine-based inhibitory motif superfamily, and its functional role is suggested to be an inhibitory receptor that modulates immunoreceptor tyrosine-based activation motif-dependent signaling cascades. In this study, we hypothesized that PECAM-1 plays an essential *in vivo* role as a counterregulator of immediate hypersensitivity reactions. We found that PECAM-1 was highly expressed on the surface of immature bone marrow mast cells and at a lower density on mature peritoneal mast cells. Examination of skin biopsies from PECAM-1<sup>+/+</sup> and PECAM-1<sup>-/-</sup> mice revealed that absence of PECAM-1 did not affect mast cell development or the capacity of mast cells to populate tissues. To examine whether the absence of PECAM-1 would influence immediate hypersensitivity reactions, PECAM-1<sup>+/+</sup> and PECAM-1<sup>-/-</sup> mice were presensitized with anti-DNP mouse IgE and then challenged 20 h later with DNP-BSA or PBS. PECAM-1<sup>-/-</sup> mice exhibited elevated serum histamine concentrations after Ag stimulation compared with PECAM-1<sup>+/+</sup> mice, indicating an increased severity of systemic IgE-mediated anaphylaxis. PECAM-1<sup>-/-</sup> mice have increased sensitivity to local cutaneous IgE-dependent anaphylaxis compared with PECAM-1<sup>+/+</sup> mice, as assessed by greater tissue swelling of their ears and mast cell degranulation *in situ*. PECAM-1<sup>-/-</sup> bone marrow mast cells showed enhanced dense granule serotonin release after FcεRI cross-linking *in vitro*. These results suggest that PECAM-1 acts as a counterregulator in allergic disease susceptibility and severity and negatively modulates mast cell activation. *The Journal of Immunology*, 2002, 168: 6455–6462.

Current therapeutic strategies for the treatment of allergic diseases involve the avoidance of allergens and the use of anti-inflammatory drugs, including corticosteroids and antihistamines (1). Although anti-inflammatory drugs can be effective in treating allergic conditions, they are often associated with systemic side effects. Recently, administration of a humanized murine mAb directed against the FcεRI binding domain of FcεRI (recombinant human Ab E25) in atopic individuals has shown promising results. This mAb functions by decreasing serum IgE to almost undetectable levels and reduces the early phase (mast cell-mediated) and late phase (inflammation-mediated) responses to inhaled allergen (2). An alternative therapeutic option being explored is targeting the molecular mechanisms that function as negative regulators of the early phase of mast cell activation. These include the inhibitory coreceptors that contain intracytoplasmic immunoreceptor tyrosine-based inhibitory motifs (ITIMs).<sup>3</sup> Mast cells

contain several Ig-ITIM-bearing receptors, including the low-affinity IgG receptor FcγRIIB, transmembrane glycoprotein receptor gp49B1, signal regulatory protein (SIRP) $\alpha$ , mast cell function-associated Ag, and platelet endothelial cell adhesion molecule-1 (PECAM-1)/CD31 (3–7). These inhibitory coreceptors can inhibit mast cell activation by ITIM-mediated recruitment and activation of distinct Src homology 2 domain-containing protein-tyrosine phosphatase (SHP)-1 and/or SHP-2 or Src homology 2 domain-containing inositol polyphosphate 5'-phosphatase (SHIP)1 and/or SHIP2 (5). Adoption of the active configuration of phosphatases exposes their catalytic active site necessary for dephosphorylation of the  $\beta$ - and  $\gamma$ -chains of FcεRI and other substrates to block the activation signals generated via cross-linking the FcεRIs when allergen is bound to cell surface IgE. During an allergic response, stimulation of the FcεRI pathway induces release of vasoactive substances from dense granules, including histamine and serotonin, and synthesis and release of cytokines. A major problem underlying FcεRI-mediated signaling in mast cells is to define the mechanisms that control direct feedback counterregulatory pathways that dampen the early phase of mast cell activation pathway following FcεRI engagement.

Generation of mouse models in which mast cell coreceptors have been deleted by gene targeting strategies has provided new insights into the regulation of FcεRI-mediated mast cell activation *in vivo* and *in vitro*. Mice deficient in mast cell coreceptors, FcγRIIB, and gp49B1 exhibit increased vascular permeability and systemic and local IgE-dependent anaphylactic responses (8, 9).

Division of Hematology, Hanson Institute, Institute of Medical and Veterinary Science, Adelaide, South Australia, Australia

Received for publication February 25, 2002. Accepted for publication April 17, 2002.

The costs of publication of this article were defrayed in part by the payment of page charges. This article must therefore be hereby marked *advertisement* in accordance with 18 U.S.C. Section 1734 solely to indicate this fact.

<sup>1</sup> This work was supported by funding from Asthma South Australia and the National Health and Medical Research Council of Australia. M.-X.W. is a postgraduate student of the University of South Australia. D.E.J. is the recipient of an National Health and Medical Research Council R. Douglas Wright Fellowship.

<sup>2</sup> Address correspondence and reprint requests to Dr. Denise E. Jackson, Division of Hematology, Hanson Institute, Institute of Medical and Veterinary Science, Frome Road, Adelaide, South Australia 5000, Australia. E-mail address: Denise.Jackson@imvs.sa.gov.au

<sup>3</sup> Abbreviations used in this paper: ITIM, immunoreceptor tyrosine-based inhibitory motif; PECAM-1, platelet endothelial cell adhesion molecule-1; BMMC, bone marrow mast cell; SIRP, signal regulatory protein; SHP, Src homology 2 domain-containing protein-tyrosine phosphatase; SHIP, Src homology 2 domain-containing inositol polyphosphate 5'-phosphatase.

Fc $\gamma$ RIIB-deficient mice also display increased vascular permeability in passive cutaneous IgG-dependent anaphylaxis (10). This increase in severity of anaphylactic responses in Fc $\gamma$ RIIB and gp49B1 mice reflects the fact that these mast cell coreceptors are essential to provide a direct negative feedback regulation of Fc $\epsilon$ RI signaling. Fc $\gamma$ RIIB has a single ITIM and selectively uses SHIP upon coaggregation with immune complexes to delivery inhibitory signaling events (11). In contrast, gp49B1 has two ITIMs and preferentially recruits SHP-1 following Ab-mediated coligation of gp49B1 to Fc $\epsilon$ RI, inhibiting IgE-induced mast cell activation *in vitro* (12).

PECAM-1 is a newly assigned member of the Ig superfamily with six extracellular Ig domains and two cytosolic ITIMs (13–16). PECAM-1 is highly expressed at the lateral junctions of endothelial cells and at a lower density on the surfaces of neutrophils, monocytes, platelets, NK cells, T and B cell subsets, and mast cells. PECAM-1 has been demonstrated to be involved in neutrophil recruitment *in vivo*, neutrophil and monocyte chemotaxis, and transendothelial migration of monocytes and neutrophils *in vitro* (17–19). Anti-domain 1 PECAM-1 mAbs and soluble PECAM-IgG chimeric molecules have been shown to inhibit transmigration of leukocytes through endothelium and *in vivo* neutrophil recruitment (17, 18, 20–22).

Studies in rat mucosal mast cells (RBL-2H3 cell line) have shown that PECAM-1 becomes tyrosine phosphorylated and preferentially recruits SHP-2 following Fc $\epsilon$ RI engagement (7, 23). However, no functional data are available on the ability of PECAM-1 to modulate mast cell activation either *in vitro* or *in vivo*. SHP-2 has been implicated in both positive and negative signaling pathways, depending upon the cell type and signaling complexes formed (24). Analysis of chimeric receptors expressing the extracellular portion of Fc $\gamma$ RIIB and intracellular portion of SIRP $\alpha$  (a known SHP-2-binding receptor) in RBL-2H3 cell line has revealed that the cytoplasmic domain of SIRP $\alpha$  is sufficient to inhibit IgE-induced mediator secretion and cytokine synthesis in mast cells *in vitro* (5). Additional studies will be required to precisely define the functional role of PECAM-1 and SHP-2 in mast cell function.

Because no naturally occurring deficiency of PECAM-1 has been reported in humans, the availability of PECAM-1-deficient mice provides us with the opportunity to directly test the functional importance of PECAM-1 in local and systemic IgE-dependent anaphylaxis *in vivo* and mast cell secretory responses of primary bone marrow mast cells (BMMC) *in vitro*. PECAM-1<sup>-/-</sup> mice are born at the expected mendelian frequency and remain viable and healthy throughout life (25). To test the hypothesis that PECAM-1 acts as a counterregulator in allergic disease susceptibility and severity, we examined the local cutaneous and passive systemic IgE-dependent anaphylaxis responses of PECAM-1-deficient mice compared with wild-type mice. To complement these studies, we tested whether primary cultured BMMC from wild-type and PECAM-1<sup>-/-</sup> mice showed any functional differences in mast cell mediator secretion responses *in vitro*.

## Materials and Methods

### Mice

The construction of the PECAM-1-deficient mice has been previously described in detail (25). These PECAM-1-deficient mice have been further backcrossed six generations onto C57BL/6 background. All mice were housed under pathogen-free conditions in a specific pathogen-free barrier-protected animal house facility at Adelaide University (Adelaide, South Australia). The phenotype of wild-type and PECAM-1-deficient mice was confirmed by flow cytometry analysis of peripheral blood elements using a monoclonal rat anti-mouse PECAM-1 390 Ab directed against Ig domain 2 (a gift from Dr. S. Albelda, University of Pennsylvania Medical Center, Philadelphia, PA) (26).

### Derivation of primary BMMC lines

Bone marrow cells were derived from 4- to 8-wk-old femurs of PECAM-1<sup>+/+</sup> and PECAM-1<sup>-/-</sup> mice and were cultured in IL-3-containing BMMC complete medium containing DMEM, 10% FCS, 50% WEHI-3DB<sup>-</sup> conditioned medium, 2 mM L-glutamine, 100  $\mu$ M nonessential amino acids, 1 mM sodium pyruvate, and 10<sup>-5</sup> M 2-ME as described (12). After 4–5 wk, >97% of suspension cells in the cultures were confirmed as immature mast cells by toluidine blue staining and flow cytometry analysis with specific mast cell markers, including IgE receptor and c-Kit staining.

### Isolation of peritoneal mast cells

Peritoneal mast cells were isolated from 10 wild-type mice by washing with Tyrode's buffer containing gelatin and purification through sequential 22% (w/v) metrizamide gradients (Sigma-Aldrich, St. Louis, MO) (27). Using this procedure, purified peritoneal mast cells were obtained at >95% purity as assessed by Fc $\epsilon$ RI expression.

### Flow cytometric analysis

Single cell suspensions (1  $\times$  10<sup>6</sup> cells/ml) of BMMC were single stained with Abs directed against a range of Ags including IgE receptor (anti-DNP mouse IgE, clone SPE-7; Sigma-Aldrich), c-Kit (Ack2; a gift from L. Ashman, Hanson Institute, Adelaide, South Australia, Australia) (28) and PECAM-1 (390). Abs were biotinylated and detected with streptavidin-R-PE (Southern Biotechnology Associates, Birmingham, AL) or detected with labeled secondary Abs, anti-rat R-PE (Southern Biotechnology Associates). Data were collected on an Epic XL-MCL (Beckman Coulter, Fullerton, CA) and analyzed using WinMDI version 2.8 software (copyright 1993–1998, J. Trotter; <http://facs.scripps.edu/software.html>).

### Preparation of monomeric IgE

Commercial preparations of anti-DNP mouse IgE mAb (clone SPE-7; Sigma-Aldrich) were subjected to ultracentrifugation and the supernatants were further purified by Sepharose gel filtration column chromatography before use. Freshly prepared monomeric IgE was used in all our studies.

### Skin mast cell determination

Sections of skin were removed from the ears and back of PECAM-1<sup>+/+</sup> and PECAM-1<sup>-/-</sup> mice. These tissue samples were fixed in 10% formalin and embedded in paraffin. Five-micrometer sections were cut and stained with Giemsa stain. The number of tissue mast cells was counted in both skin sections derived from the ears and back of PECAM-1<sup>+/+</sup> and PECAM-1<sup>-/-</sup> mice at  $\times$ 40 magnification across six high-power fields on an Olympus BH-2 microscope (Olympus, Phillips, Australia).

### Active systemic anaphylaxis

PECAM-1<sup>+/+</sup> and PECAM-1<sup>-/-</sup> mice were *i.v.* injected with 3  $\mu$ g anti-DNP mouse IgE (Sigma-Aldrich). Twenty-four hours later, mice were challenged with *i.v.* administration of 500  $\mu$ g of DNP-BSA (Sigma-Aldrich) or PBS. After 1.5 min, mice were sacrificed by CO<sub>2</sub> inhalation and blood was immediately collected by cardiac puncture. Serum was isolated from blood samples and tested for serum histamine concentration by competitive histamine ELISA (Immunotech, Marseille, France).

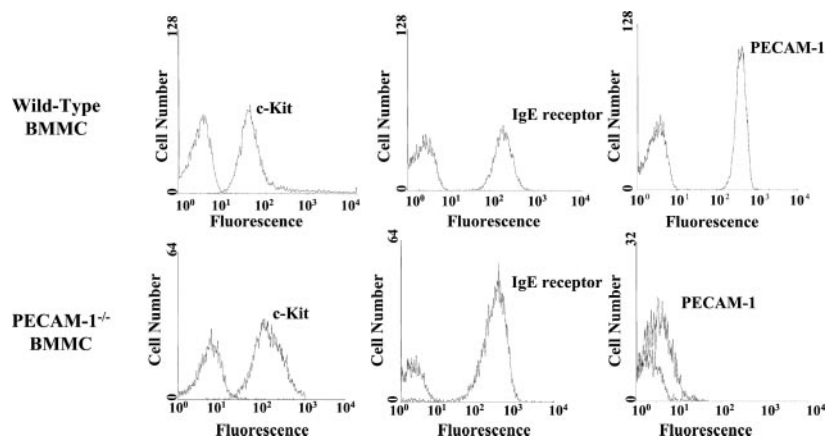
### Local cutaneous anaphylaxis

The left and right ears of 5-wk-old PECAM-1<sup>+/+</sup> and PECAM-1<sup>-/-</sup> mice were intradermally injected with either 20  $\mu$ l of PBS or 10 ng anti-DNP mouse IgE (clone SPE-7; Sigma-Aldrich). Twenty hours later, the mice were challenged with an *i.v.* injection of 500  $\mu$ g DNP-BSA (Sigma-Aldrich) or PBS. Ear thickness measurements were recorded at 0.5, 1, 2, 4, and 8 h using a dial thickness gauge (Mitutoyo, Tokyo, Japan) with a minimum sensitivity of 1  $\mu$ m. Net ear thickness was determined as the difference between the thicknesses of the right and left ears of each mouse.

### Histology

In some local cutaneous anaphylaxis experiments, PECAM-1<sup>+/+</sup> and PECAM-1<sup>-/-</sup> mice were sacrificed 30 min after administration with DNP-BSA. Left and right ears were removed, fixed in 10% formalin, and embedded in paraffin. Five-micrometer sections were cut and then stained with Giemsa stain. Intact and degranulated tissue mast cells were counted by examining at  $\times$ 40 magnification using an Olympus BH-2 microscope. A degranulated mast cell was defined as a cell showing release of >10% cell granules.

**FIGURE 1.** Surface FcεRI, c-Kit, and PECAM-1 expression in wild-type and PECAM-1<sup>-/-</sup> BMMC. BMMC from wild-type and PECAM-1<sup>-/-</sup> mice were characterized after 4–5 wk of culture in IL-3-containing WEHI-3-conditioned medium. BMMC were stained with biotinylated anti-DNP mouse IgE or biotinylated anti-mouse PECAM-1 390 Ab, and binding was detected with streptavidin-R-PE. c-Kit expression was detected with rat anti-mouse c-Kit (Ack2) Ab followed by anti-rat-R-PE. Isotype-matched IgG Abs were used as appropriate negative controls. Data analysis was performed on an EPICS XL-MCL flow cytometer and viable BMMC were defined by their forward and side scatter characteristics. Representative histograms of BMMC from wild-type and PECAM-1<sup>-/-</sup> mice are shown.



### Electron microscopy

For conventional electron microscopy, BMMCs were fixed with a mixture of 2% paraformaldehyde and 1% glutaraldehyde in 0.2 M cacodylate buffer (pH 7.4), postfixed with 1% OsO<sub>4</sub> supplemented with 15% ferrocyanide, dehydrated in ethanol, and embedded in Epon. Ultrathin sections were viewed with a TEM CM120 Philips electron microscope (Philips Electronic Systems, Mahwah, NJ) after counterstaining with uranyl acetate and lead citrate.

### Degranulation

The degree of dense granule secretion was determined by measuring the release of serotonin. PECAM-1<sup>+/+</sup> and PECAM-1<sup>-/-</sup> BMMC (1 × 10<sup>7</sup> cells/ml) were preloaded with 1 μCi 5-hydroxy [<sup>3</sup>H]tryptamine trifluoroacetate (without IL-3; Amersham Pharmacia Biotech, Little Chalfont, U.K.) overnight in a CO<sub>2</sub> incubator at 37°C. Cells were washed once in Tyrode's buffer (112 mM NaCl, 2.7 mM KCl, 0.4 mM NaH<sub>2</sub>PO<sub>4</sub>, 1.6 mM CaCl<sub>2</sub>, 1 mM MgCl<sub>2</sub>, 10 mM HEPES (pH 7.5), 0.05% (w/v) gelatin, 0.1% (w/v) glucose) and resuspended in 200 μl of Tyrode's buffer. For stimulating with IgE alone, 10 μg/ml anti-DNP mouse IgE (without IL-3; Sigma-Aldrich) was incubated with cells at 37°C for 15 min. For stimulation with IgE plus polyvalent Ag, DNP-BSA, cells were incubated with 10 μg/ml anti-DNP mouse IgE for 2 h at 37°C. Washed cells were stimulated with varying doses of DNP-BSA (0–100 ng/ml) and incubated for 15 min at 37°C. As a positive control, cells were incubated with 10 μM ionomycin/20 ng/ml PMA for 15 min at 37°C as a check on the integrity of the cell signaling machinery. Samples were centrifuged at 4000 rpm for 5 min, supernatants were separated, and cell pellets were solubilized in 0.5% Triton X-100 (Sigma-Aldrich, St. Louis, MO). The release of serotonin was measured in triplicate by liquid scintillation in both cell supernatants and pellets and calculated as a percentage of degranulation. The percentage of release values were calculated using the formula [(S/S + P) × 100], where S and P are the serotonin contents of the supernatants and pellet, respectively, from each sample.

### Statistical analysis

Numerical values were expressed as the mean ± SD. Experimental results were evaluated by two-way ANOVA to allow comparison of data obtained from PECAM-1<sup>+/+</sup> and PECAM-1<sup>-/-</sup> mice at different time points. In some cases, the Student *t* test was used to analyze experimental data at the same time point in the time course.

## Results

### PECAM-1 deficiency does not affect mast cell development or capacity of mast cells to populate tissues

The generation and preliminary characterization of PECAM-1<sup>-/-</sup> mice have been previously reported (25). Functional assessment of *in vitro* platelet-collagen responses has revealed that the PECAM-1<sup>-/-</sup> mice have phenotypic features of an inhibitory receptor knockout (29). In this study, we sought to test the possibility that PECAM-1 may serve an essential role as a counterregulator of allergic disease susceptibility and severity. In initial studies, we demonstrated by flow cytometry that PECAM-1 is highly expressed on the surface of immature BMMC derived from bone marrow of PECAM-1<sup>+/+</sup> mice, but not in PECAM-1<sup>-/-</sup> BMMC (Fig. 1). We also showed that PECAM-1 was expressed at a lower density on the surface of mature peritoneal mast cells compared with immature BMMC (Fig. 2).

Given the essential role for PECAM-1 in transbasement migration (25), we wanted to investigate whether absence of PECAM-1 would have any detrimental effect on the capacity of tissue mast cells to populate tissues. To test this possibility, skin was removed from the ears and back of PECAM-1<sup>+/+</sup> and PECAM-1<sup>-/-</sup> mice,

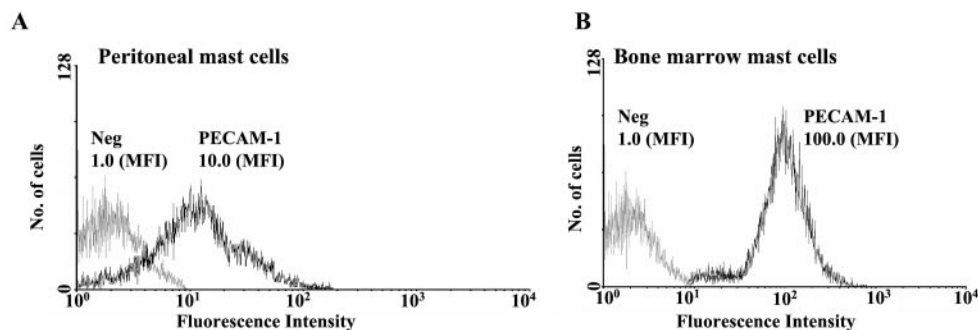


**FIGURE 2.** PECAM-1 expression on the surface of BMMC and peritoneal mast cells. A total of 1 × 10<sup>6</sup> cells/ml purified peritoneal mast cells (A) and wild-type BMMC (B) were stained with biotinylated anti-mouse PECAM-1 390 Ab, and binding was detected with streptavidin-R-PE. An isotype-matched IgG Ab was used as a negative control. Data analysis was performed on an EPICS XL-MCL flow cytometer and viable cells were defined by their forward and side scatter characteristics. MFI, Mean fluorescence intensity.



and 5- $\mu\text{m}$  Giemsa-stained sections were examined and quantitated for tissue mast cell content by light microscopy. As shown in Fig. 3, there was no significant difference (Student's *t* test;  $p > 0.05$ ;  $n = 6$ ) in the number of tissue skin mast cells derived from the ears and back of PECAM-1<sup>+/+</sup> and PECAM-1<sup>-/-</sup> mice. Collectively, these data suggest that PECAM-1 is expressed in mast cells and is not required for mast cell development and populating tissues.

#### Passive systemic IgE-dependent anaphylaxis is enhanced in PECAM-1<sup>-/-</sup> mice

Passive systemic IgE-dependent anaphylaxis is dependent upon passive transfer of anti-DNP mouse IgE Ab followed by i.v. administration of the cross-linking polyvalent Ag, DNP-BSA. Mice deficient in FcεRIα, Src homology 2 domain-containing leukocyte phosphoprotein-76, linker for activation of T cells, Gab2, and mast cell-deficient WBB6F1-W/W<sup>v</sup> all lead to diminished or virtually absent systemic IgE-dependent anaphylactic responses (30–35), while mice deficient in FcγRIIB and gp49B1 show enhanced systemic IgE-dependent anaphylactic responses (8, 9). These studies in gene-targeted mice reveal the importance of components of the FcεRI pathway together with the presence of mast cells and inhibitory receptors in modulating susceptibility to IgE-dependent anaphylaxis.

To test the *in vivo* function of PECAM-1 in passive systemic IgE-dependent anaphylaxis, we challenged PECAM-1<sup>+/+</sup> and PECAM-1<sup>-/-</sup> mice with an i.v. administration of 3  $\mu\text{g}$  monoclonal anti-DNP mouse IgE, then (24 h later) with 500  $\mu\text{g}$  DNP-BSA or PBS. After 1.5 min mice were sacrificed, blood was collected, and serum was isolated for determination of histamine concentration. As shown in Fig. 4, IgE stimulation alone did not induce an increase in serum histamine concentration in PECAM-1<sup>-/-</sup> mice compared with PECAM-1<sup>+/+</sup> mice. In contrast, PECAM-1<sup>+/+</sup> mice showed an increase in serum histamine concentration upon FcεRI cross-linking, while PECAM-1<sup>-/-</sup> mice showed a significant elevation in serum histamine concentration (6,565  $\pm$  2,363 nM vs 12,985  $\pm$  3,569 nM; Student's *t* test;  $p < 0.001$ ;  $n = 13$ ). These results are consistent with our hypothesis that the absence of PECAM-1 as an inhibitory receptor leads to more severe passive systemic IgE-dependent anaphylaxis.

#### Local cutaneous IgE-dependent anaphylaxis is enhanced in PECAM-1<sup>-/-</sup> mice

To determine whether PECAM-1 serves as a negative regulator of FcεRI mast cell activation in local cutaneous anaphylaxis, the left and right ears of PECAM-1<sup>+/+</sup> and PECAM-1<sup>-/-</sup> mice were injected intradermally with 20  $\mu\text{l}$  PBS or 10 ng anti-DNP mouse IgE. Twenty hours later, mice were challenged with 500  $\mu\text{g}$  DNP-BSA or PBS by i.v. tail vein injection. Left and right ear tissue swelling was monitored at various time points from  $t = 0.5, 1, 2, 4,$  and 8 h

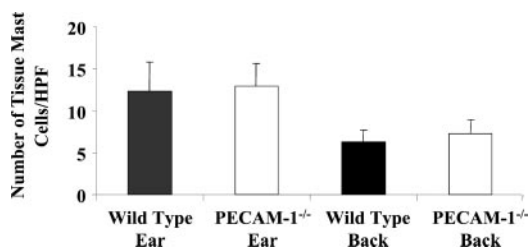


**FIGURE 3.** PECAM-1 is not required for mast cell development. Skin was removed from the ears and back of PECAM-1<sup>+/+</sup> ( $n = 6$ ) and PECAM-1<sup>-/-</sup> ( $n = 6$ ) mice, and 5- $\mu\text{m}$  Giemsa-stained sections were examined and quantitated for tissue mast cell content by light microscopy at  $\times 40$  magnification on an Olympus BH-2 microscope.

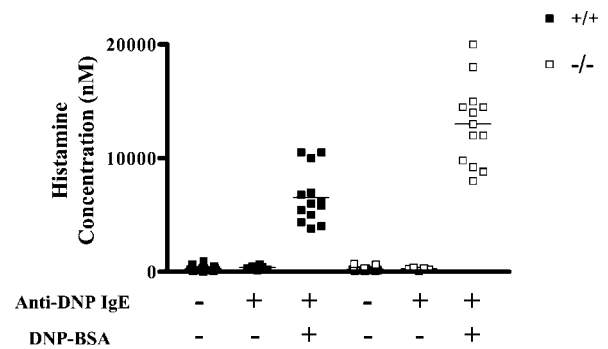


**FIGURE 4.** IgE-mediated systemic anaphylaxis in PECAM-1<sup>-/-</sup> mice. PECAM-1<sup>+/+</sup> (■;  $n = 13$ ) and PECAM-1<sup>-/-</sup> (□;  $n = 13$ ) mice were sensitized with 3  $\mu\text{g}$  anti-DNP mouse IgE by i.v. injection. Twenty-four hours later, mice were challenged with 500  $\mu\text{g}$  DNP-BSA or PBS; after 1.5 min, mice were sacrificed and blood was collected for determination of serum histamine concentration. Results represent serum histamine concentrations of PECAM-1<sup>+/+</sup> and PECAM-1<sup>-/-</sup> mice with and without Ag stimulation. The mean values of each group are indicated.

with a dial thickness gauge. As shown in Fig. 5, the net ear thickness for PECAM-1<sup>-/-</sup> mice was significantly increased compared with PECAM-1<sup>+/+</sup> mice following FcεRI mast cell activation induced by IgE anti-DNP and cross-linking with DNP-BSA (Student's *t* test;  $p < 0.001$ ;  $n = 6$ ). The net ear swelling peaked at 1 h and slowly subsided by 2 h. Following induction of Ag-dependent IgE-mediated local anaphylaxis, a 10-fold increase in net ear thickness was observed for PECAM-1<sup>-/-</sup> mice (Fig. 5B) when compared with Ag-independent IgE/PBS control at peak swelling of 1 h (Fig. 5A). In contrast, PECAM-1<sup>+/+</sup> mice showed a 4-fold

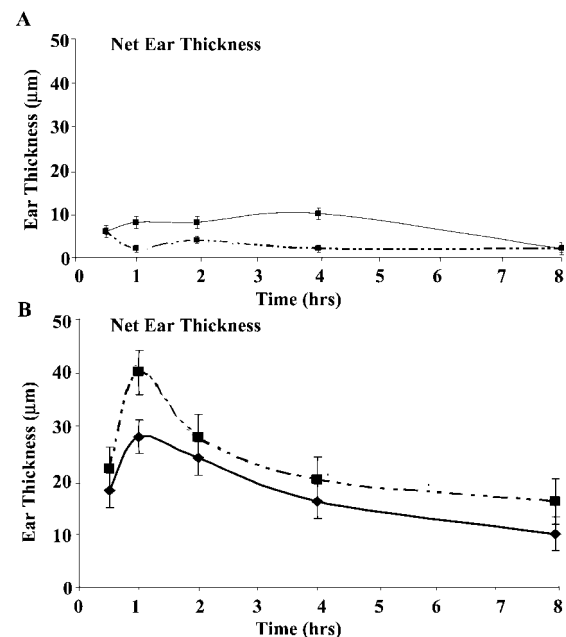


**FIGURE 5.** IgE-mediated local cutaneous anaphylaxis in PECAM-1<sup>-/-</sup> mice. The ears of PECAM-1<sup>+/+</sup> ( $n = 6$ ) and PECAM-1<sup>-/-</sup> ( $n = 6$ ) mice were intradermally injected with either 20  $\mu\text{l}$  of PBS (left ear) or 10 ng anti-DNP mouse IgE (right ear). Twenty hours later, the mice were challenged with an i.v. injection of PBS (A) or 500  $\mu\text{g}$  DNP-BSA (B). Ear thickness measurements were recorded at 0.5, 1, 2, 4, and 8 h using a dial thickness gauge. These measurements account for the degree of ear swelling in wild-type (solid line) and PECAM-1<sup>-/-</sup> (dashed line) mice. Net ear thickness was determined as the difference between the thicknesses of the right and left ears of each mouse.

increase in net ear thickness compared with Ag-independent IgE/PBS control at peak swelling of 1 h. Importantly, we observed that the net ear thickness was higher in PECAM-1<sup>-/-</sup> mice at all times compared with PECAM-1<sup>+/+</sup> mice. To examine the numbers of intact vs degranulated tissue mast cells in PECAM-1<sup>+/+</sup> and PECAM-1<sup>-/-</sup> mice during local cutaneous IgE-dependent anaphylaxis, the left and right ears of PECAM-1<sup>+/+</sup> and PECAM-1<sup>-/-</sup> mice were injected intradermally with 20  $\mu$ l PBS or 10 ng anti-DNP mouse IgE. Twenty hours later, mice were challenged with 500  $\mu$ g DNP-BSA by i.v. tail vein injection. In these experiments, mice were sacrificed at  $t = 0.5$  h, ears were removed, and 5- $\mu$ m Giemsa-stained sections were examined and quantitated for intact tissue mast cell content by light microscopy. The right ears of PECAM-1<sup>-/-</sup> mice showed 4-fold fewer intact tissue mast cells 0.5 h after challenge compared with PECAM-1<sup>+/+</sup> mice, as demonstrated in histological sections (Fig. 6A) and by quantitation of intact tissue mast cells (Student's  $t$  test;  $p < 0.005$ ;  $n = 5$ ) (Fig. 6B). Importantly, tissue mast cells in skin tissue sections of PECAM-1<sup>-/-</sup> mice displayed quantitatively more degranulation than comparative samples from wild-type mice (Student's  $t$  test;  $p < 0.005$ ;  $n = 5$ ) (Fig. 6C). These results suggest that PECAM-1 serves as a negative regulator in dampening local cutaneous anaphylaxis, which is a hallmark feature of bee stings, insect bites, and latex hypersensitivity.

*BMMC from PECAM-1<sup>-/-</sup> mice are hyperresponsive in degranulation and secretory responses following Fc $\epsilon$ RI cross-linking in vitro*

To investigate the underlying mechanism responsible for the increased severity of PECAM-1<sup>-/-</sup> mice to local and systemic IgE-mediated anaphylaxis due to defective Fc $\epsilon$ RI-mediated degranulation of mast cells, we next examined the capacity of wild-type and PECAM-1<sup>-/-</sup> BMMC to degranulate by examining their response to anti-DNP IgE stimulation alone and anti-DNP IgE stimulation with varying doses of DNP-BSA and PMA/ionomycin. After 4–5 wk in culture, the various BMMC lines expressed >95% Fc $\epsilon$ RI expression (Fig. 1) and showed comparable staining of metachromatic granules with toluidine blue or alcian blue-safranin (data not shown). Electron microscopy studies of the various BMMC lines revealed similar cell morphology, membrane projections, presence of cytoplasmic morphologically distinct granules including internal vesicles (type I), granules with an electron-dense core surrounded by membrane vesicles (type II), and electron-dense granules (type III) (Fig. 7A) (36). Examination of the ultrastructural components of various BMMC phenotypes by transmission electron microscopy enabled quantitation of type III electron-dense granule content in primary murine BMMC derived from PECAM-1<sup>+/+</sup> and PECAM-1<sup>-/-</sup> mice. Quantitation of dense

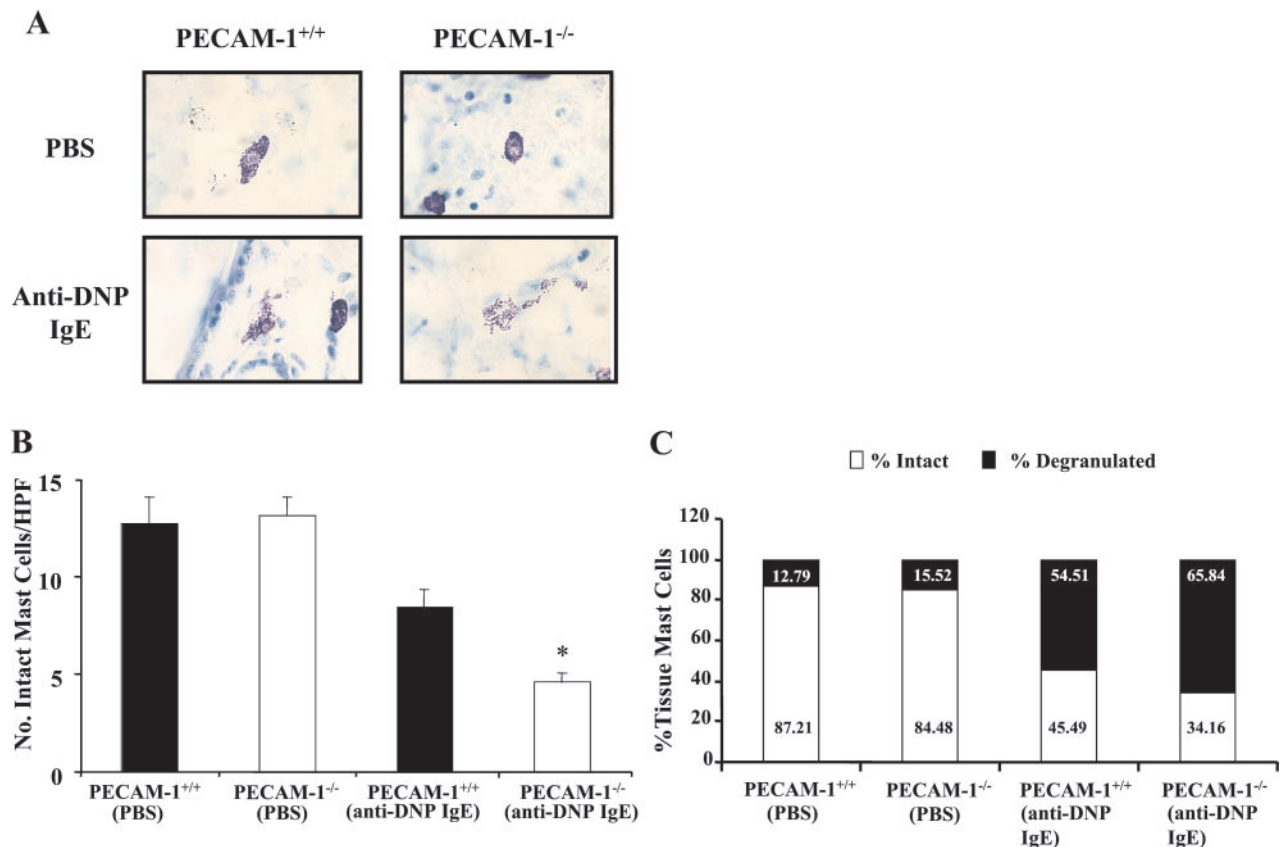


**FIGURE 6.** Enhanced degranulation of mast cells in situ in PECAM-1<sup>-/-</sup> mice during IgE-mediated local cutaneous anaphylaxis. *A*, Experimental conditions essentially as outlined in Fig. 5. At  $t = 0.5$  h, mice were sacrificed, ears were removed, and 5- $\mu$ m Giemsa-stained sections were examined by light microscopy. PECAM-1<sup>+/+</sup> ( $n = 5$ ) and PECAM-1<sup>-/-</sup> ( $n = 5$ ) tissue sections are shown for PBS and anti-DNP mouse IgE to show intact and degranulated tissue mast cells. All photographs represent similar magnifications, time exposures, and camera settings. *B*, Quantitation of intact mast cells was defined by punctuate staining of metachromatic cytoplasmic granules surrounding an intact nucleus per high-power field in tissue sections from ears of PECAM-1<sup>+/+</sup> and PECAM-1<sup>-/-</sup> mice, 0.5 h after Ag challenge. *C*, Quantitation of skin mast cells were calculated by counting the number of intact vs degranulated cells in four different 5- $\mu$ m Giemsa-stained sections derived from PECAM-1<sup>+/+</sup> ( $n = 5$ ) compared with PECAM-1<sup>-/-</sup> ( $n = 5$ ) mice under light microscopy. Magnification,  $\times 40$ . The results are expressed as the mean. Note that the number of degranulated mast cells was significantly higher in PECAM-1<sup>-/-</sup> mice (Student's  $t$  test;  $p < 0.005$ ).

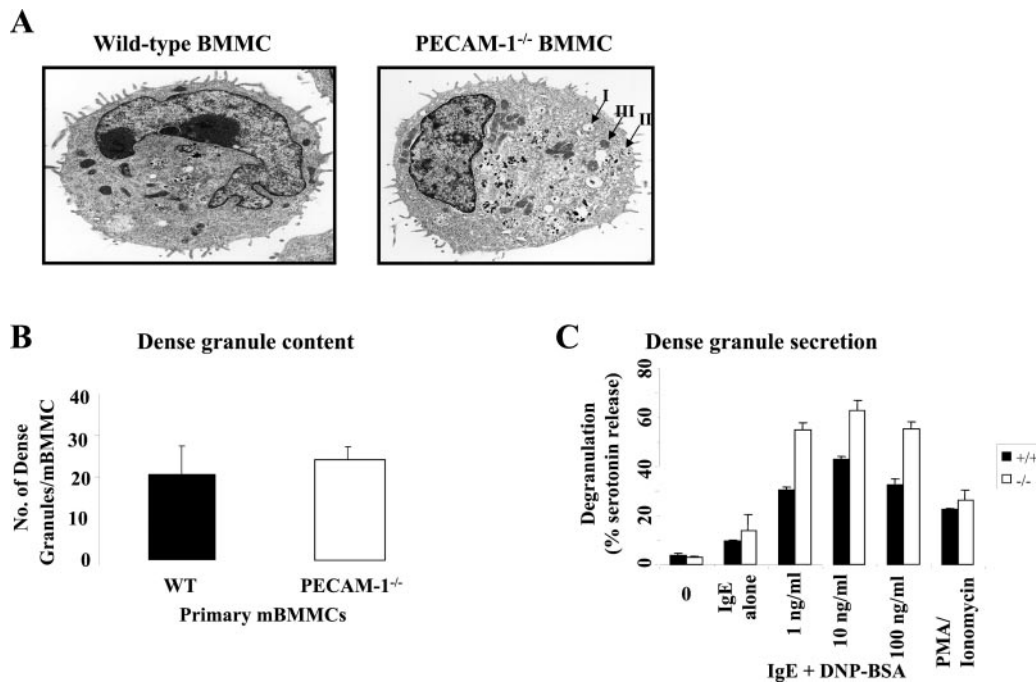


**FIGURE 7.** Enhanced FcεRI-mediated serotonin release in PECAM-1<sup>-/-</sup> BMMC. **A**, Transmission electron micrographs of representative BMMC from wild-type and PECAM-1<sup>-/-</sup> mice. Magnification,  $\times 3000$ . Note that PECAM-1<sup>-/-</sup> BMMC have normal morphology, membrane projections, and presence of cytoplasmic dense granules. Cytoplasmic granules included internal vesicles (type I), granules with an electron-dense core surrounded by membrane vesicles (type II), and electron-dense granules (type III). All photographs represent similar magnifications, time exposures, and camera settings. **B**, Quantitation of the numbers of dense granules per cultured BMMC for wild-type and PECAM-1<sup>-/-</sup> mice. **C**, PECAM-1<sup>+/+</sup> and PECAM-1<sup>-/-</sup> BMMC were labeled with [<sup>3</sup>H]serotonin, then sensitized with anti-DNP mouse IgE alone or a combination of anti-DNP mouse IgE with varying doses of DNP-BSA (0–1000 ng/ml) and PMA (20 ng/ml) plus ionomycin (10  $\mu$ M). Serotonin released in the supernatant and associated with the cell pellet was quantitated by scintillation counting. Data are expressed as a percentage of total counts (supernatant/supernatant + pellet  $\times 100\%$ ) released and are the average of triplicate samples. These data are representative of at least three independent experiments.

granules from each of the BMMC lines revealed comparable numbers of type III electron-dense granules per BMMC (Student's *t* test;  $p > 0.05$ ;  $n = 15$ ) (Fig. 7B). As the dense granule content was comparable between the primary murine BMMC lines, we then wanted to correlate the *in vivo* studies of local and systemic anaphylaxis with mast cell degranulation *in vitro*. As shown in Fig. 7C, FcεRI-evoked degranulation (as indicated by serotonin release) was markedly enhanced in PECAM-1<sup>-/-</sup> BMMC. The PECAM-1<sup>+/+</sup> BMMC consistently released  $\sim 42\%$  of their total granule contents, whereas the PECAM-1<sup>-/-</sup> BMMC released 65% of their total granule contents following stimulation with anti-DNP IgE and FcεRI cross-linking with DNP-BSA. Dose-dependent curves revealed a peak of degranulation at concentrations of 10 ng/ml DNP-BSA for all cell lines tested. In contrast, PMA plus ionomycin-induced degranulation was comparable in wild-type and PECAM-1<sup>-/-</sup> BMMC. Therefore, our results suggest that the secretion machinery in PECAM-1<sup>-/-</sup> BMMC is intact but the absence of PECAM-1 leads to defective hyperresponsive FcεRI-mediated degranulation. Our observation that FcεRI cross-linking induces enhanced degranulation in PECAM-1<sup>-/-</sup> BMMC suggests that the presence of PECAM-1 in mast cells plays an important role in preventing inappropriate mast cell degranulation.

## Discussion

The high incidence of allergic disorders affecting the developed world has prompted studies into the field of immune inhibitory receptors to explore direct feedback counterregulatory mechanisms in adaptive immediate hypersensitivity reactions. In these studies, we have investigated the functional importance of a newly classified member of the Ig-ITIM superfamily, PECAM-1, in mod-

ulating *in vivo* and *in vitro* IgE-mediated allergic reactions using PECAM-1-deficient mice and primary BMMC lines derived from PECAM-1-deficient mice. Our studies suggest that PECAM-1 plays a key role in negatively regulating Ag-dependent IgE-mediated mast cell activation. Importantly, the absence of PECAM-1 did not affect mast cell development and the capacity of mast cells to populate tissues (Fig. 3). PECAM-1<sup>-/-</sup> mice displayed a hyperresponsive phenotype in Ag-dependent IgE-mediated passive systemic anaphylaxis (Fig. 4) and local cutaneous anaphylaxis (Figs. 5 and 6), which is suggestive of an inhibitory receptor knockout phenotype.

Systemic anaphylaxis is a health condition whereby the individual succumbs to a severe allergic reaction to a specific allergen. Because it is regarded as a reflection of extensive mast cell activation (32), we decided to assess the severity of this allergic condition in wild-type and PECAM-1<sup>-/-</sup> mice. We chose to evaluate a passive rather than active method of sensitization to exclude the participation of other Ab classes, which may complicate the comparison and interpretation of the anaphylactic responses. Sensitization of mice for active anaphylaxis induces not only an IgE response but also production of Ag-specific IgG1 Abs (37), which can participate (with IgE Abs) in both local cutaneous anaphylaxis (8) and passive systemic anaphylactic responses (38). Passive sensitization ensures sole activation of FcεRI-containing mast cells and basophils that have been primed with anti-DNP IgE and receptor cross-linked with DNP-BSA. As previously mentioned, there was a marked enhancement of systemic anaphylaxis in PECAM-1<sup>-/-</sup> mice when compared with their wild-type counterparts, which was quantitatively assessed by a sensitive serum histamine assay. This hyperresponsive phenotype is consistent with



the *in vivo* findings obtained from Fc $\gamma$ RIIB<sup>-/-</sup> mice (8). In gp49B1<sup>-/-</sup> mice, systemic anaphylaxis was measured by enhanced mast cell degranulation in the trachea and also increased mortality (68 vs 27%) in a shorter time frame (26 vs 45 min) when compared with their wild-type counterparts (9). In contrast, mice that were deficient in Fc $\epsilon$ RI $\alpha$ , linker for activation of T cells, Src homology 2 domain-containing leukocyte phosphoprotein-76, Vav, and Gab2 have shown decreased serum histamine concentrations when compared with normal serum histamine levels (32–35). Under these circumstances, the results are indicative of mast cell insufficiency to degranulate, thus attenuating effector function. Thus, these findings indicate that the activatory components of the Fc $\epsilon$ RI signaling pathway are crucial in IgE-mediated allergic responses. Conversely, as shown by PECAM-1<sup>-/-</sup>, Fc $\gamma$ RIIB<sup>-/-</sup>, and gp49B1<sup>-/-</sup> mice, abrogation of the inhibitory receptor leads to enhanced systemic anaphylaxis where there is extensive mast cell degranulation and death.

The medical condition of local IgE-dependent reactions is highly prevalent in the developed world. It is characterized by typical local allergic responses to insect stings, latex-induced hypersensitivity, and other allergenic substances, such as pollen. A local allergic response is commonly reflected by localized swelling at particular sites of tissue within the body. Taking this important indicator of local anaphylaxis into account, we devised experiments in which to assess the effect of PECAM-1 in regulation of local cutaneous anaphylaxis. Upon induction of local cutaneous anaphylaxis, we found that PECAM-1<sup>-/-</sup> mice exhibited a 2- to 3-fold greater ear swelling at 1 h following Ag-dependent challenge with IgE and DNP-BSA compared with their wild-type counterparts. In both genotypes of mice, a peak net ear swelling was observed after 1 h of Ag challenge which eventually subsided and returned to basal levels by 8 h. The observations in the PECAM-1<sup>-/-</sup> mice share features comparable with gp49B1<sup>-/-</sup> mice, which displayed a 2- to 3-fold greater net swelling at 0.5–2 h after Ag challenge when compared with their wild-type counterparts (9). To investigate whether there was a correlation between these observational findings and mast cell degranulation, ear tissue from wild-type and PECAM-1<sup>-/-</sup> mice were removed 30 min after the induction of IgE-mediated local cutaneous anaphylaxis and were examined histologically. As defined by tissue histology, the number of morphologically intact mast cells was significantly reduced 3-fold in the Ag-challenged PECAM-1<sup>-/-</sup> mice at 0.5 h. This finding was also comparable to gp49B1<sup>-/-</sup> mice, which displayed a 2-fold decrease in intact mast cells at both 0.5- and 4-h time points (9). To further substantiate these suggestions of extensive mast cell degranulation, intact and degranulated mast cells within the skin of Ag-challenged PECAM-1<sup>-/-</sup> mice were quantitated and were demonstrated to contain a higher percentage of degranulated mast cells when compared with wild-type mice. Hence, these findings are indicative of an enhanced susceptibility to IgE-mediated mast cell degranulation in inhibitory receptor knockout animals.

Previous studies in rat mucosal mast cells, RBL-2H3 cells, have revealed that PECAM-1 becomes tyrosine phosphorylated upon Fc $\epsilon$ RI aggregation with anti-Fc $\epsilon$ RI $\alpha$  receptor Abs and recruits the protein-tyrosine phosphatase, SHP-2 (7, 23). At this time, no studies were reported that examined the functional importance of PECAM-1 in regulating Fc $\epsilon$ RI-evoked mast cell responses. Functional studies were also impeded by the lack of naturally occurring PECAM-1-deficient human individuals, thus prompting us to use genetically altered PECAM-1-deficient mice to directly assess the functional importance of PECAM-1 in mast cell activation *in vivo* and *in vitro*. Importantly, because the Fc $\epsilon$ RI is intrinsic to multiple cell types, including mast cells and basophils, it was imperative to

conduct *in vitro* studies on IL-3-dependent primary BMMC populations derived from wild-type and PECAM-1<sup>-/-</sup> mice to determine whether PECAM-1 plays an essential role in regulating Fc $\epsilon$ RI-mediated signaling pathways. Our *in vitro* studies revealed that PECAM-1 is highly expressed on the surface of immature murine bone marrow-derived mast cell progenitors but at a lower density on the surface of mature peritoneal mast cells (Figs. 1 and 2). PECAM-1<sup>-/-</sup> primary BMMC exhibited normal morphology, equivalent type III dense granule content, and similar kinetics of growth (data not shown) compared with wild-type BMMC (Fig. 7). PECAM-1<sup>-/-</sup> primary BMMC showed hyperresponsive features of Ag-dependent IgE-mediated mast cell activation, as indicated by elevated Fc $\epsilon$ RI-evoked secretion of dense granule serotonin following IgE stimulation and DNP-BSA cross-linking compared with wild-type BMMC (Fig. 7).

This Ag-dependent Fc $\epsilon$ RI-mediated hyperresponsive mast cell phenotype observed in PECAM-1<sup>-/-</sup> BMMC was not observed in other inhibitory receptor knockouts, including Fc $\gamma$ RIIB<sup>-/-</sup> BMMCs and gp49B1<sup>-/-</sup> BMMC (10, 39). Loss of Fc $\gamma$ RIIB rendered the cells sensitive to IgG-mediated triggering but did not have a substantial effect on Fc $\epsilon$ RI-mediated activation (10). In contrast, loss of gp49B1 in BMMC did not result in any difference in hypersensitivity in Ag-dependent IgE-mediated mast cell activation (40). These results appear to conflict with the *in vivo* enhanced systemic and local cutaneous anaphylaxis observed in the gp49B1<sup>-/-</sup> mice (9). The reason for this discrepancy between the *in vivo* and *in vitro* data is not clear and further studies are required to resolve this issue.

In summary, immune inhibitory mechanisms are equally as important as immune system activation. Classical symptoms of cellular hyperresponsiveness, including autoimmunity and anaphylaxis, are evident in mice that possess targeted disruptions of their inhibitory receptors. In this study, we have defined PECAM-1 as a new mast cell coreceptor that provides a direct feedback mechanism to negatively attenuate Ag-dependent IgE/Fc $\epsilon$ RI-mediated signal transduction. By studying the mechanism by which we can manipulate IgE-FcR interactions, we can identify potential novel and more-effective avenues of prophylactic treatment for allergy.

## Acknowledgments

We thank Dr. Tak Mak and Dr. Gordon Duncan (Amgen Institute, Toronto, Ontario, Canada) for the generation of the PECAM-1<sup>-/-</sup> mice. We also thank Dr. Steve Albelda for the supply of rat anti-mouse PECAM-1 390 Ab.

## References

- Barnes, P. J. 1999. Therapeutic strategies for allergic diseases. *Nature* 402:B31.
- Patalano, F. 1999. Injection of anti-IgE antibodies will suppress IgE and allergic symptoms. *Allergy* 54:103.
- Benhamou, M., C. Bonnerot, W. H. Fridman, and M. Daeron. 1990. Molecular heterogeneity of murine mast cell Fc $\gamma$  receptors. *J. Immunol.* 144:3071.
- Katz, H. R., A. C. Benson, and K. F. Austen. 1989. Activation- and phorbol ester-stimulated phosphorylation of a plasma membrane glycoprotein antigen expressed on mouse IL-3-dependent mast cells and serosal mast cells. *J. Immunol.* 142:919.
- Lienard, H., P. Bruhns, O. Malbec, W. H. Fridman, and M. Daeron. 1999. Signal regulatory proteins negatively regulate immunoreceptor-dependent cell activation. *J. Biol. Chem.* 274:32493.
- Ortega Soto, E., and I. Pecht. 1988. A monoclonal antibody that inhibits secretion from rat basophilic leukemia cells and binds to a novel membrane component. *J. Immunol.* 141:4324.
- Sagawa K., W. Swaim, J. Zhang, E. Unsworth, and R. P. Siraganian. 1997. Aggregation of the high affinity IgE receptor results in the tyrosine phosphorylation of the surface adhesion protein PECAM-1 (CD31). *J. Biol. Chem.* 272:13412.
- Ujike, A., Y. Ishikawa, M. Ono, T. Yuasa, T. Yoshino, M. Fukumoto, J. V. Ravetch, and T. Takai. 1999. Modulation of immunoglobulin (Ig) E-mediated systemic anaphylaxis by low-affinity Fc receptors for IgG. *J. Exp. Med.* 189:1573.



9. Daheshia, M., D. S. Friend, M. J. Grusby, K. F. Austen, and H. R. Katz. 2001. Increased severity of local and systemic anaphylactic reactions in gp49B1-deficient mice. *J. Exp. Med.* 194:227.
10. Takai, T., M. Ono, M. Hikida, H. Ohmori, and J. V. Ravetch. 1996. Augmented humoral and anaphylactic responses in Fc $\gamma$ R2-deficient mice. *Nature* 379:346.
11. Ono, M., S. Bolland, P. Tempst, and J. V. Ravetch. 1996. Role of the inositol phosphatase SHP in negative regulation of the immune system by the receptor Fc $\gamma$ R2B. *Nature* 383:263.
12. Katz, H. R., E. Vivier, M. C. Castells, M. J. McCormick, J. M. Chambers, and K. F. Austen. 1996. Mouse mast cell gp49B1 contains two immunoreceptor tyrosine-based inhibition motifs and suppresses mast cell activation when co-ligated with the high-affinity Fc receptor for IgE. *Proc. Natl. Acad. Sci. USA* 93:10809.
13. Jackson, D. E., C. M. Ward, R. Wang, and P. J. Newman. 1997. The protein-tyrosine phosphatase SHP-2 binds platelet/endothelial cell adhesion molecule-1 (PECAM-1) and forms a distinct signaling complex during platelet aggregation: evidence for a mechanistic link between PECAM-1 and integrin-mediated cellular signaling. *J. Biol. Chem.* 272:6986.
14. Jackson, D. E., K. R. Kupcho, and P. J. Newman. 1997. Characterization of phosphotyrosine binding motifs in the cytoplasmic domain of platelet/endothelial cell adhesion molecule-1 (PECAM-1) that are required for the cellular association and activation of the protein-tyrosine phosphatase, SHP-2. *J. Biol. Chem.* 272:24868.
15. Hua, C. T., J. R. Gamble, M. A. Vadas, and D. E. Jackson. 1998. Recruitment and activation of SHP-1 protein-tyrosine phosphatase by human platelet endothelial cell adhesion molecule-1 (PECAM-1): identification of immunoreceptor tyrosine-based inhibitory motif-like binding motifs and substrates. *J. Biol. Chem.* 273:28332.
16. Newman, P. J. 1999. Switched at birth: a new family for PECAM-1. *J. Clin. Invest.* 103:5.
17. Vaporciyan, A. A., H. M. DeLisser, H. C. Yan, I. I. Mendiguren, S. R. Thom, M. L. Jones, P. A. Ward, and S. M. Albelda. 1993. Involvement of platelet-endothelial cell adhesion molecule-1 in neutrophil recruitment in vivo. *Science* 262:1580.
18. Bogen, S., J. Pak, M. Garifallou, X. Deng, and W. A. Muller. 1994. Monoclonal antibody to murine PECAM-1 (CD31) blocks acute inflammation in vivo. *J. Exp. Med.* 179:1059.
19. Muller, W. A., S. A. Weigl, X. Deng, and D. M. Phillips. 1993. PECAM-1 is required for transendothelial migration of leukocytes. *J. Exp. Med.* 178:449.
20. Liao, F., J. Ali, T. Green, and W. A. Muller. 1997. Soluble domain 1 platelet-endothelial cell adhesion molecule (PECAM) is sufficient to block transendothelial migration in vitro and in vivo. *J. Exp. Med.* 185:1349.
21. Liao, F., A. R. Schenkel, and W. A. Muller. 1999. Transgenic mice expressing different levels of soluble platelet/endothelial cell adhesion molecule-IgG display distinct inflammatory phenotypes. *J. Immunol.* 163:5640.
22. Nakada, M. T., K. Amin, M. Christofidou-Solomidou, C. D. O'Brien, J. Sun, I. Gurubhagavatula, G. A. Heavner, A. H. Taylor, C. Paddock, Q.-H. Sun, et al. 2000. Antibodies against the first Ig-like domain of human platelet endothelial cell adhesion molecule-1 (PECAM-1) that inhibit PECAM-1-dependent homophilic adhesion block in vivo neutrophil recruitment. *J. Immunol.* 164:452.
23. Sagawa, K., T. Kimura, M. Swieter, and R. P. Siraganian. 1997. The protein-tyrosine phosphatase SHP-2 associates with tyrosine-phosphorylated adhesion molecule PECAM-1 (CD31). *J. Biol. Chem.* 272:31086.
24. Timms, J. F., K. D. Swanson, A. Marie-Cardine, M. Raab, C. E. Rudd, B. Schraven, and B. G. Neel. 1999. SHPS-1 is a scaffold for assembling distinct adhesion regulated multi-protein complexes in macrophages. *Curr. Biol.* 9:927.
25. Duncan, G. S., D. P. Andrew, H. Takimoto, S. A. Kaufman, H. Yoshida, J. Spellberg, J. Lius de la Pompa, A. Elia, A. Wakeham, B. Karan-Tamir, et al. 1999. Genetic evidence for functional redundancy of platelet endothelial cell adhesion molecule-1 (PECAM-1/CD31) CD31-deficient mice reveal PECAM-1-dependent and PECAM-1-independent functions. *J. Immunol.* 162:3022.
26. DeLisser, H. M., M. Christofidou-Solomidou, R. M. Strieter, M. D. Burdick, C. S. Robinson, R. S. Wexler, J. S. Kerr, C. Garlanda, J. R. Merwin, J. A. Madri, and S. M. Albelda. 1997. Involvement of endothelial PECAM-1/CD31 in angiogenesis. *Am. J. Pathol.* 151:671.
27. Price, J. A. Two-layer gradient isolation of rat peritoneal mast cells. 1997. *Bio-Techniques* 22:616.
28. Ogawa, M., Y. Matsuzaki, S. Nishikawa, S. Hayashi, T. Kunisada, T. Sudo, H. Nakauchi, and S. Nishikawa. 1999. Expression and function of c-Kit in hemopoietic progenitor cells. *J. Exp. Med.* 174:63.
29. Jones, K. L., S. C. Hughan, S. M. Doppeide, R. W. Farndale, S. P. Jackson, and D. E. Jackson. 2001. Platelet endothelial cell adhesion molecule-1 (PECAM-1/CD31) is a negative regulator of platelet-collagen interactions. *Blood* 98:1456.
30. Takeishi, T., T. R. Martin, I. M. Katona, F. D. Finkelman, and S. J. Galli. 1991. Differences in the expression of the cardiopulmonary alterations associated with anti-immunoglobulin E-induced or active anaphylaxis in mast cell-deficient and normal mice: mast cells are not required for the cardiopulmonary changes associated with certain fatal anaphylactic responses. *J. Clin. Invest.* 88:598.
31. Martin, T. R., A. Ando, T. Takeishi, I. M. Katona, J. M. Drazen, and S. J. Galli. 1993. Mast cells contribute to the changes in heart rate, but not hypotension or death, associated with active anaphylaxis in mice. *J. Immunol.* 151:367.
32. Dombrowicz, D., V. Flamand, K. K. Brigman, B. H. Koller, and J. P. Kinet. 1993. Abolition of anaphylaxis by targeted disruption of the high affinity immunoglobulin E receptor  $\alpha$  chain gene. *Cell* 75:969.
33. Pivniouk, V. I., T. R. Martin, J. M. Lu-Kuo, H. R. Katz, H. C. Oettgen, and R. S. Geha. 1999. SLP-76 deficiency impairs signaling via the high-affinity IgE receptor in mast cells. *J. Clin. Invest.* 103:1737.
34. Saitoh, S., R. Arudchandran, T. S. Manetz, W. Zhang, C. L. Sommers, P. E. Love, J. Rivera, and L. E. Samelson. 2000. LAT is essential for Fc $\epsilon$ R1-mediated mast cell activation. *Immunity* 12:525.
35. Gu, H., K. Saito, L. D. Klaman, J. Shen, T. Fleming, Y. Wang, J. C. Pratt, G. Lin, B. Lim, J. P. Kinet, and B. G. Neel. 2001. Essential role for Gab2 in the allergic response. *Nature* 412:186.
36. Raposo, G., D. Tenza, S. Mecheri, R. Peronet, C. Bonnerot, and C. Desaymard. 1997. Accumulation of major histocompatibility complex II molecules in mast cell secretory granules and their release upon degranulation. *Mol. Biol. Cell* 8:2631.
37. Finkelman, F. D., I. M. Katona, J. F. Urban, and W. E. Paul. 1989. Control of in vivo IgE production in the mouse by interleukin 4. *Ciba Found. Symp.* 147:3.
38. Harada, M., M. Nagata, T. Takeuchi, T. Ohara, S. Makino, and A. Watanabe. 1991. Age-dependent difference in susceptibility to IgE antibody- and IgG1 antibody-mediated passive anaphylactic shock in the mouse. *Immunol. Invest.* 20:515.
39. Rojo, S., C. C. Stebbins, M. E. Peterson, D. Dombrowicz, N. Wagtmann, and E. O. Long. 2000. Natural killer cells and mast cells from gp49B null mutant mice are functional. *Mol. Cell. Biol.* 20:7178.
40. Metcalfe, D. D., D. Baram, and Y. A. Mekori. 1997. Mast cells. *Physiol. Rev.* 77:1033.